Development of Resistance to the Atypical Retinoid, ST1926, in the Lung Carcinoma Cell Line H460 Is Associated with Reduced Formation of DNA Strand Breaks and a Defective DNA Damage Response[1]

Valentina Zuco, Chiara Zanchi*, Cinzia Lanzi*, Giovanni L. Beretta*, Rosanna Supino*, Claudio Pisano†, Marcella Barbarino†, Romina Zanier†, Federica Bucci†, Concetta Aulicino†, Paolo Carminati† and Franco Zunino**

*Istituto Nazionale per lo Studio e la Cura dei Tumori, Milan 20133, Italy; †Sigma-Tau, Rome 00040, Italy

Abstract

Atypical retinoids are potent inducers of apoptosis, but activation of the apoptotic pathway seems to be independent of retinoid receptors. Previous studies with a novel adamantyl retinoid, ST1926, have shown that apoptosis induction is associated with an early genotoxic stress. To better understand the relevance of these events, we have selected a subline of the H460 lung carcinoma cell line resistant to ST1926. Resistant cells exhibited cross-resistance to a related molecule, CD437, but not cross-resistance to agents with different mechanisms of action. In spite of a lack of defects in intracellular drug accumulation, induction of DNA strand breaks in resistant cells required exposure to a substantially higher concentration, which was consistent with the degree of resistance. At drug concentrations causing a similar antiproliferative effect (IC_{80}) and a comparable extent of DNA lesions in sensitive and resistant cells, the apoptotic response was a delayed and less marked event in resistant cells, thus indicating a reduced susceptibility to apoptosis. In spite of recognition of DNA lesions in resistant cells, as supported by phosphorylation of p53 and histone H2AX, resistant cells exhibited no activation of the mitochondrial pathways of apoptosis. Following exposure to equitoxic drug concentrations, only sensitive cells exhibited a typical stress/DNA damage response, with activation of the S-phase checkpoint. The cellular resistance to ST1926 reflects alterations responsible for a reduced generation of DNA lesions and for an enhanced tolerance of the genotoxic stress, resulting in lack of activation of the intrinsic pathway of apoptosis. The defective DNA damage response, accompanied by a reduced susceptibility to apoptosis in resistant cells, provides further support to the involvement of genotoxic stress as a critical event in mediating apoptosis induction by ST1926.

Neoplasia (2005) **7,** 667–677

Keywords: atypical retinoids, cellular resistance, apoptosis, DNA damage, stress response.

Introduction

The pharmacologic interest of retinoids in cancer therapy and chemoprevention is related to their ability to modulate a variety of critical biologic functions including cell growth and differentiation. Whereas the broad biologic effects of classic retinoids are mediated by retinoid receptors [1], the antiproliferative and proapoptotic activities of novel synthetic retinoid-related molecules (RRMs or atypical retinoids) are described to be independent of receptor-mediated transcriptional activity [2,3]. The best known compound belonging to this class of proapoptotic RRMs is CD437, which was reported to be selective for RARγ [4]. Although a number of potential targets for drug action have been identified and several aspects of drug-induced apoptosis have been elucidated, the molecular mechanism of action of RRMs is only partially understood [2–5]. The intrinsic apoptotic pathway involving mitochondrial damage has been implicated in CD437-induced apoptosis [6]. Cellular effects of atypical retinoids also involve p53 activation and a p53-dependent increase of cell death receptors and, therefore, the activation of extrinsic pathway of apoptosis [7]. However, it is likely that multiple pathways are implicated in the apoptotic action of atypical retinoids and the contribution of different events may be dependent on the cellular context [2,5]. A better understanding of the molecular events mediating the inhibition of cell growth and apoptosis induction by atypical retinoids could provide a rational basis for the design of more effective treatments also in combination with other agents.

Recently, a related compound of this series, ST1926, was found to be a potent inducer of apoptosis in a large panel of human tumor cells and showed efficacy against solid tumor models derived from human ovarian carcinoma, lung carcinoma, and melanoma at well-tolerated doses [8,9]. The increased antiproliferative and apoptogenic potency of ST1926,

Address all correspondence to: Franco Zunino, Istituto Nazionale Tumori, *Via* Venezian 1, Milan 20133, Italy. E-mail: franco.zunino@istitutotumori.mi.it

[1]This work was partially supported by the Associazione Italiana Ricerca sul Cancro (Milan), Ministero della Salute (Rome), and CNR-MIUR (Rome, Italy).

Received 13 January 2005; Revised 25 March 2005; Accepted 29 March 2005.

DOI 10.1593/neo.05127

compared to CD437, in spite of a modest RAR activation supports the view that the cellular effects of the novel agent are independent of retinoid receptors [9,10].

The pattern of cellular response to the adamantyl retinoid, ST1926, suggested that the induction of genotoxic stress was implicated in mediating drug-induced apoptosis [9]. To identify the critical determinants of cellular sensitivity to ST1926, we characterized a lung carcinoma cell line, H460/ST1926 (R9A), which was selected following continuous *in vitro* exposure to ST1926. A comparison of the extent of DNA lesions and of the cellular response in parental and resistant cells to ST1926 is consistent with a critical role of DNA damage response in determining cell fate and suggests that tolerance to drug-induced genotoxic stress contributes to resistance status.

Materials and Methods

Cell Lines and Culture Conditions

The human lung carcinoma cell line, H460, and its subline, R9A, selected for resistance to ST1926, were maintained in RPMI 1640 (Bio-Whittaker, Verviers, Belgium) supplemented with 10% FBS (Life Technologies, Inc., Gaithersburg, MD). The R9A subline was selected by culturing cells for 6 months in culture medium containing 2 μM ST1926. R9A cells were subcultured in the absence of the drug and a resistance index (ratio between the IC_{50} of resistant and sensitive cells) of 200 was maintained for at least 3 months. Both sensitive and resistant cells were characterized by wild-type p53.

Drugs and Antibodies

ST1926 (synthesized as described by Cincinelli et al. [8]) and CD437 were supplied by Prof. L. Merlini (DISMA, University of Milan, Italy). Stock solutions of ST1926 and CD437 were prepared in dimethylsulfoxide (DMSO) and stored at −20°C, prior to further dilution in culture medium. The highest final concentration of DMSO in culture medium was 0.5%. Doxorubicin (Pharmacia UpJohn, Milan, Italy) was dissolved in water; paclitaxel (Indena, Milan, Italy) and ZD1839 (Astra Zeneca, Manlesfield, Cheshire, UK) were dissolved in DMSO; and cisplatin (Platinex) (Bristol Myers Squibb, Rome, Italy) was dissolved in 0.9% NaCl before use.

Killer-TRAIL was supplied by Alexis Biochemicals (Lausen, Switzerland). Lonidamine (LND) (Angelini, Rome, Italy) was dissolved in 2.3% *N*-methyl-D-glucamine (NMG) and further diluted in water to a final concentration of 3.2 mg/ml immediately prior to use.

The following antibodies were used: anti−phospho-p38 MAP kinase (Thr 180/Tyr 182) and anti−phospho-p44/42 MAP kinase (Thr 202/Tyr 204) (New England Biolaboratories, Beverly, MA); anti−phospho-JNK (Thr 183/Tyr 185), anti-p38 (C-20), and anti-p73 (E-4) (Santa Cruz Biotechnology, Santa Cruz, CA); anti-MAPK 1/2 (ERK 1/2-CT) and anti−γ-H2AX (Upstate Biotechnology, Lake Placid, NY); anti−phospho-Akt (Ser473), anti−SAPK/JNK, anti−cleaved caspase-3, and anti−phospho-p53 (Ser15) (Cell Signaling Technology, Beverly, BA); anti−PBKα/Akt (Transduction Laboratories, Lexington, KY); anti-p53 and anti−Bcl-2 (Dako, Glostrup, Denmark); anti-p21, anti−RPA-2, and anti−caspase-9 (NeoMarker, Union City, CA); anti-BAX and anti−caspase-8 (BD Pharmigen/Becton Dickinson, Mountain View, CA); anti−PARP-1 (Oncogene Science, Uniondale, NY); anti−cytochrome *C* (BD Pharmigen/Becton Dickinson); and anti-actin (Sigma, St. Louis, MO).

Cell Sensitivity Studies

Cell sensitivity to drugs was determined by growth inhibition assay. Cells were seeded in duplicate into six-well plates and exposed to γ-rays or to the drugs for 24 hours (ST1926) or 72 hours (ST1926, CD437, paclitaxel, ZD1839, and LND). In all cases, adherent cells were trypsinized and counted 72 hours after the beginning of treatment by a cell counter (Coulter Electronics, Luton, UK). IC_{50} values, derived from dose−response curves, were defined as drug concentrations producing 50% inhibition of cell growth. The reported values represents the mean ± standard deviation (SD) of at least three independent experiments.

The effect of the combination of ST1926 with TRAIL on cell growth was assessed by sulforhodamine B (SRB) assay. Cells were seeded in 96-well plate and incubated for 24 hours with ST1926 or TRAIL alone or in combination. After 48 hours from drug removal, cells were subjected to SRB staining. Drug interactions, expressed as combination index (CI) values, were calculated according to the following formula:

$$CI = \frac{(SFa \times SFb)}{SF(a+b)} / 100$$

where SF indicates the survival fraction observed with each drug (*a* and *b*) or with the cotreatment (*a* + *b*). According to the analysis described by Drewinko et al. [11], CI values indicate the following interaction: CI > 1, synergism; CI = 1, additivity; CI < 1, antagonism.

Drug Uptake

The intracellular drug content was measured following incubation of the cells with 0.3 μM ST1926 for 1 hour. Cells were then washed with phosphate-buffered saline (PBS) and incubated in drug-free medium for different time intervals to measure drug retention. Cells were lysed in PBS containing 0.1% sodium dodecyl sulphate (SDS) and ST1926 was extracted two times by ethylacetate. The organic phase was dried in a nitrogen flux and the pellet was resuspended in ethanol. Samples were left for 2 hours at −20°C and then centrifuged. Supernatants were analyzed by HPLC (Beckman Instruments, Fullerton, CA). The separation was performed by isocratic elution (80% methanol, 0.02% trifluoroacetic acid), with a flow rate of 1 ml/min on a LiChroCART4-4/Lichrospher 100 RP-18, 5 μm (Merck, Whitehouse Station, N.J.). The detection was performed with a spectrofluorimetric detector RF-10A_{XL} Shimadzu at λ_{exc} 330 nm and λ_{em} 475 nm. All data were expressed as mean (ng ST1926 / mg total proteins) ± SD.

Cell Cycle Analysis

Cells were exposed to drug concentrations corresponding to the IC_{80} value calculated after 72 hours of treatment (i.e., 0.2 and 20 μM for H460 and R9A cells, respectively). At different times, cells were washed, fixed in ice-cold 70% ethanol, and stored at −20°C. After rehydration in PBS, cellular DNA was stained with 10 μg/ml propidium iodide (PI) (Sigma) in PBS containing RNase A (66 U/ml) (Sigma), for 18 hours. Cell cycle distribution was determined by a FACScan flow cytometer (Becton Dickinson) and data were analysed by Cell Quest software. At least 10,000 cells were analyzed for DNA content.

Detection of Apoptosis

Apoptosis was detected by terminal deoxynucleotidyl transferase–mediated deoxyuridine triphosphate nick-end labelling (TUNEL assay) and annexin V staining.

For the TUNEL assay, cells were fixed in 4% paraformaldehyde, for 60 minutes, at room temperature, washed, and resuspended in ice-cold PBS. The In Situ Cell Death Detection Kit Fluorescein (Roche, Mannheim, Germany) was used according to the manufacturers' instructions and the samples were analysed by flow cytometry using Cell Quest software (Becton Dickinson). For the annexin reaction, cells (1×10^5) were suspended in 100 μl of binding buffer (10 mM HEPES–NaOH, pH 7.4, 140 mM NaCl, 2.5 mM $CaCl_2$), 5 μl of annexin V–FITC (BD Pharmigen/Becton Dickinson), and 5 μl of PI (final concentration, 1 μg/ml) for 15 minutes. After the addition of 400 μl of binding buffer, cells were analysed on a FACScan.

Alkaline Elution Assay

DNA single-strand breaks were detected by the alkaline elution method [12]. Cells were incubated in the presence of 0.08 μCi/ml [^{14}C]thymidine (Amersham Biosciences, Amersham, UK) for 30 hours, and then for 18 hours in the absence of labeled thymidine to chase the DNA-incorporated radioactivity. After treatment with different concentrations of ST1926 for 6 hours, cells were immediately processed for alkaline elution as previously described [9]. A positive control consisting of cells irradiated with 0.4 Gy was used as a reference.

Immunofluorescence Staining of γ-H2AX

H460 and R9A cells were seeded on slides in six-well plates and, 24 hours later, treated with ST1926 at 0.2 and 20 μM, respectively, corresponding to equitoxic (IC_{80}) concentrations, for 3 hours. At the end of treatment, cells were fixed in 2% paraformaldehyde in PBS for 5 minutes, washed in PBS, permeabilized in 100% methanol at −20°C for 20 minutes, and blocked with PBS containing 1% bovine serum albumin and 0.1% Tween 20 (PBA) for 15 minutes. Then, samples were incubated with anti–γ-H2AX mouse monoclonal antibody for 1 hour, followed by AlexaFluor 594–conjugated goat antimouse antibody (Molecular Probes, Eugene, OR) for 1 hour. Slides were then washed in PBA, incubated with 2 mg/ml Hoechst 33341 (Sigma) for 2 minutes, mounted with Mowiol, and examined by a fluorescence microscope.

Western Blot Analysis

Cells were rinsed twice with cold PBS added with 0.1 mM sodium orthovanadate and lysed in hot sample buffer [9]. After determination of protein concentration, whole-cell extracts were separated by SDS polyacrylamide gel electrophoresis (PAGE) and transferred onto nitrocellulose filters. The filters were incubated with primary antibodies overnight and with peroxidase-conjugated secondary antibodies at room temperature for 1 hour. Immunoreactive bands were revealed by using the enhanced chemiluminescence detection system from Amersham Biosciences or Pierce (Rockford, IL).

Measurement of Cytochrome C Release from Mitochondria

H460 and R9A cells were exposed to ST1926 (IC_{80}, 0.2 and 20 μM, respectively) or LND (IC_{80}, 155 μM) for different times. Floating and adherent cells were harvested and cytosolic extracts were prepared as described [13]. Briefly, cells were homogenized in ice-cold lysis buffer (20 mM HEPES–KOH, pH 7.5, 10 mM KCl, 1.5 mM $MgCl_2$, 1 mM EDTA, 1 mM EGTA, 250 mM sucrose, 0.5 mM phenylmethylsulfonyl fluoride, 10 μg/ml leupeptin, 10 μg/ml aprotinin, and 10 μg/ml trypsin inhibitor) by 25 strokes in a Dounce homogenizer and centrifuged at 20,000*g* for 20 minutes. Supernatants were stored at −70°C until gel electrophoresis. Cytosolic protein extracts were run on 20% SDS-PAGE and processed for Western blot analysis as described above.

Measurement of $\Delta\psi_m$ by Flow Cytometry

Mitochondrial permeability was assessed as already described [14]. H460 and R9A cells were treated for 24 hours with ST1926 at 0.2 and 20 μM, respectively. A total of 5×10^5 cells was incubated with CMTMRos (150 nM) (Molecular Probes) for 15 minutes in culture medium at 37°C and 5% CO_2. Samples were harvested, washed in PBS, and immediately analyzed by a flow cytometer (Becton Dickinson).

Analysis of Gene Expression by RT-PCR

Total cellular RNA was isolated from ST1926-treated and ST1926-untreated cells by using a commercially available kit (Talent, Trieste, Italy). Two micrograms of RNA was reversed-transcribed into cDNA by the use of oligo(dt) primers and Moloney murine leukemia virus reverse transcriptase (Invitrogen, Milan, Italy). To amplify the TR3 transcript, the 5′-tcatggacggctacacag-3′/5′-gtaggcatggaatagctc-3′primers were used. The amplified fragment was 517 bp. PCR conditions were as follows: 95°C, 9 minutes, for 1 cycle; 95°C, 1 minute, 52°C, 1 minute; 72°C, 1 minute, for 30 cycles followed by 10-minute extension at 72°C. In the case of β-actin, which was used as a control (actin primers: 5′-gaaactaccttcaactccatc-3′ and 5′-ggcggctccatcctggcctcg-3′), the annealing temperature was 62°C and the number of base pairs was 300. The amplification products were separated on 1.5% agarose gel containing ethidium bromide and

Table 1. Pattern of Cross-Resistance.

Drug	Exposure (hours)	IC_{50} (μM)*	
		H460	R9A
ST1926	24	0.21 ± 0.01	24 ± 8
ST1926	72	0.06 ± 0.03	12 ± 4.2
CD437	72	0.12 ± 0.08	>40
Doxorubicin	1	0.27 ± 0.11	0.24 ± 0.1
Cisplatin	1	19.3 ± 1.5	20 ± 3
Paclitaxel	72	0.0051 ± 0.0005	0.0035 ± 0.0003
ZD1839	72	23 ± 2	17 ± 4
γ-Ray (Gy)		2.50 ± 0.4	3.37 ± 0.67
TRAIL (ng/ml)	24	5.82 ± 1.14	1.39 ± 0.05
LND	72	118 ± 10	93 ± 10

*The antiproliferative effect was determined at 72 hours after treatment by cell counting. IC_{50} values were derived from the dose–response curves for each compound.

UV-visualized by using a VDS Image Master (Amersham Pharmacia Biotech Italia, Cologno Monzese, Italy).

Results

Pattern of Cross-Resistance

The ST1926-resistant H460 subline (R9A) exhibited a stable resistant phenotype in the absence of selective pressure. The resistance index of the subline R9A to ST1926 was very high and somewhat dependent on the exposure time (Table 1). When evaluated in terms of cell growth inhibition, the resistant subline displayed cross-resistance to CD437 but not to other antitumor agents characterized by a different mechanism of action (Table 1).

Drug Uptake

To determine whether drug resistance could be related to defects in intracellular drug accumulation, drug uptake in sensitive and resistant cells was measured following a 1-hour exposure to the same drug concentration (Figure 1). Drug uptake and retention were comparable in the two cell lines.

DNA Damage

Using the alkaline elution method, no significant extent of DNA damage could be detected in resistant cells at concentrations of ST1926 below 1 μM (i.e., at concentrations producing DNA damage and antiproliferative effects in sensitive cells). Thus, comparative studies were performed on the two cell lines after 6 hours of drug treatment in the range of cytotoxic concentrations for each cell line. As shown in Figure 2*A*, formation of DNA breaks in resistant cells required a substantially higher concentration of ST1926, but drug concentrations producing similar antiproliferative effects induced a comparable amount of DNA damage. The presence of DNA damage could be detected under these conditions by the formation of γ-H2AX foci (Figure 2*B*). H2AX phosphorylation (γ-H2AX) has been reported to be specific for the sites of DNA double-strand breaks [15,16]. This event could be detected early after treatment, as already reported for other DNA-damaging agents [17]. Indeed, γ-H2AX foci were observed in 100% of both cell lines treated with ionizing radiation (20 Gy). After a 3-hour exposure to equitoxic concentrations (IC_{80}) of ST1926, 55% of H460 and 46% of R9A cells were markedly positive for γ-H2AX staining.

RPA-2, a DNA single-strand binding protein essential for DNA replication, recombination, and repair, becomes rapidly phosphorylated after DNA damage [18]. In our cell system, RPA-2 appeared phosphorylated in H460 cells after 6 and 24 hours of exposure to ST1926, whereas a persistent downregulation of the protein was observed in the resistant cells (Figure 2*C*) following exposure to equitoxic drug concentrations (IC_{80}).

Cell Cycle Perturbation

A quite different perturbation of cell cycle progression was found in the two cell lines after treatment with equitoxic concentrations (IC_{80}) of ST1926 (Figure 3). In H460 cells, ST1926 caused a persistent accumulation of cells in the G_1/S phases. A time-dependent increase of sub-G_1 cells was consistent with the occurrence of apoptotic DNA fragmentation. The treatment caused a different profile of cell cycle distribution in resistant cells with no evidence of S-phase arrest. Resistant cells exhibited a transient accumulation in G_2 at 24 hours and a late appearance of sub-G_1 cells at 72 hours, likely reflecting cell death.

Apoptosis Induction and Caspase Activation

Figure 4 shows the extent of apoptotic cell death induced in each cell line at different exposure times to a single drug concentration corresponding to the IC_{80} (0.2 and 20 μM for H460 and R9A cells, respectively). Apoptosis induction was less marked and delayed in the resistant cells. After a 48-hour exposure, a significant level (22%) of apoptosis was detectable only in H460 cells. The different onset of apoptosis in the two cell lines was clearly documented by the annexin V binding assay, which revealed early manifestations of apoptosis in resistant cells only at 72 hours of

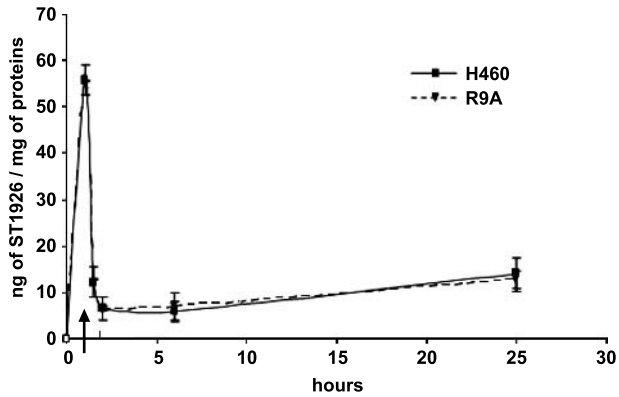

Figure 1. *Drug uptake and release of ST1926. H460 (■) and R9A (▼) cells were exposed to the same drug concentration (0.3 μM) for 1 hour. Then, cells were incubated in drug-free medium and drug retention was determined at the indicated times. The arrow indicates the end of treatment.*

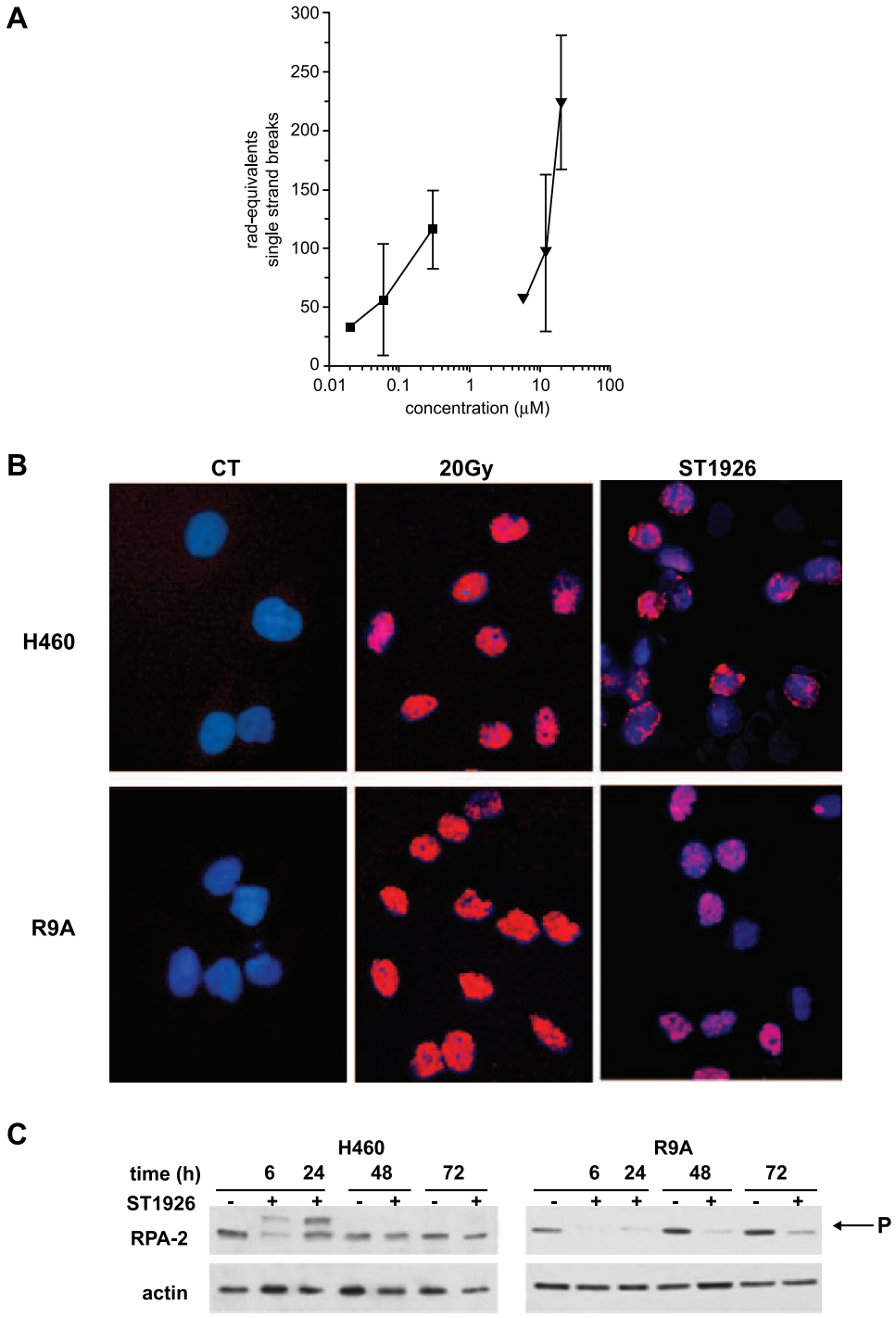

Figure 2. *Induction of DNA damage in H460 and R9A cells by ST1926. (A) DNA single-strand breaks induced by ST1926. H460 (■) and R9A (▼) cells were exposed to increasing drug concentrations for 6 hours and then DNA breaks were measured by the alkaline elution assay. The results, expressed as rad equivalents, are the mean ± SD of three independent experiments. (B) Immunofluorescence staining for γ-H2AX. Cells were treated with equitoxic concentrations (IC_{80}) of ST1926 for 3 hours and stained with mouse anti–γ-H2AX antibody and AlexaFluor 594–conjugated goat antimouse Ig second antibody (red). Nuclei were stained with Hoechst 33342 (blue). (C) RPA-2 phosphorylation following exposure to equitoxic concentrations of ST1926 (IC_{80}) for the indicated times. The arrow indicates the phosphorylated RPA-2. The results of one experiment representative of two are reported.*

treatment (Table 2). At this time, under our conditions, the treatment induced a marked antiproliferative effect in both cell lines (IC_{80}). The extent of overall apoptosis in sensitive cells could be underestimated as a consequence of early onset of apoptosis. The only moderate induction of apoptosis in R9A-resistant cells at a concentration that strongly inhibited proliferation indicated that the cytostatic activity of the drug was more pronounced than its cytotoxic activity in resistant cells compared to parental cells.

Cleavage of caspases 8, 9, and 3 was already detectable after a 24-hour exposure to ST1926 in H460 cells (Figure 5). Accordingly, a concomitant time-dependent cleavage of

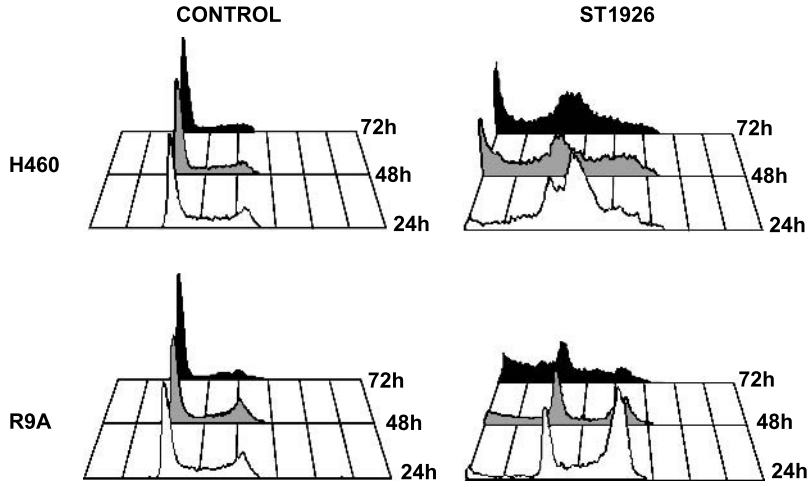

Figure 3. *Cell cycle distribution of H460-sensitive and R9A-resistant cells at different times after treatment with equitoxic concentrations of ST1926 (IC_{80}). One experiment representative of three is shown.*

PARP-1, one of the caspase substrates in apoptosis, was observed. The pattern of caspase activation was substantially different in R9A cells because no activation of caspase 9 was found at any time until 72 hours of treatment. A weak activation of caspases 3 and 8 was associated with cleavage of PARP-1, which was barely detectable starting at 24 hours of treatment. The reduced activation of caspases in R9A cells is in agreement with a lower extent of apoptosis detected by the TUNEL and annexin binding assays.

A typical mitochondrial response to proapoptotic stimuli involves the cytosolic release of cytochrome *C*, a caspase activator, and mitochondrial transmembrane depolarization [6]. Both events were detected in sensitive cells but no changes were found in the resistant cells exposed to ST1926 (IC_{80}) (Figure 6, *A* and *B*). This finding was consistent with the lack of activation of caspase 9 in resistant cells. The different mitochondrial response did not reflect a defect at mitochondrial level in resistant cells because a cytotoxic concentration (IC_{80}) of LND, a mitochondrial-targeting drug [19,20], caused the release of cytochrome *C* (Figure 6*C*), consistent with the finding that the drug induced a comparable extent of apoptosis in the two cell lines (50 ± 5% and 57 ± 10% in sensitive and resistant cells, respectively).

The resistant subline retained sensitivity to TRAIL, thus supporting no defects in the extrinsic apoptotic pathway. However, the death receptor ligand showed synergistic

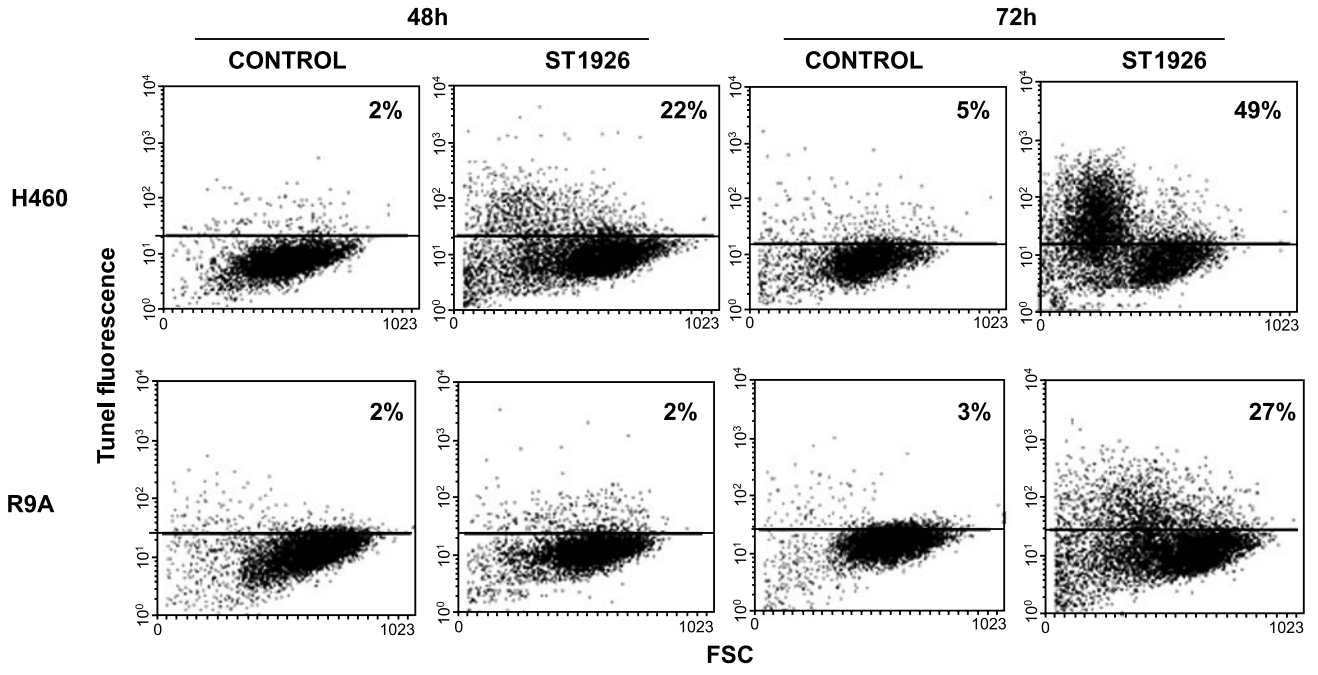

Figure 4. *Apoptosis induced by ST1926. Cells were exposed for 48 and 72 hours to 0.2 and 20 μM ST1926 corresponding to the IC_{80} value in H460 and R9A cells, respectively. Apoptosis was detected by TUNEL assay and determined by FACS analysis.*

Table 2. Apoptosis Detection by Annexin V Binding Assay in H460 and R9A Cells Treated with ST1926 (IC_{80}).

Exposure Time (hours)	H460		R9A	
	Early*	Late†	Early*	Late†
24	10 ± 3	0	3 ± 3	0
48	14 ± 4	27 ± 4	6 ± 3	9 ± 4
72	2 ± 0	48 ± 8	11 ± 4	22 ± 4

*Percentage of cells in an early stage of apoptosis (i.e., cells stained positively for annexin V–FITC and negatively for PI).
†Percentage of cells in a late stage of apoptosis (i.e., stained positively for both annexin V–FITC and PI).

interaction with ST1926 only in sensitive cells (Figure 7). This observation was consistent with a lack of activation of the mitochondrial-regulated pathway and therefore a lack of cooperation between the extrinsic and intrinsic pathways.

Modulation of Apoptosis-Related Factors

Figure 8*A* shows the expression of apoptosis-related proteins at 24, 48, and 72 hours of treatment with equitoxic concentrations (IC_{80}) of ST1926. In the parental cell line, an increase of expression of p53 and p21 was already detectable after 24 hours of treatment, together with an upregulation of Bax. In resistant cells, a less marked drug-induced upregulation of p21 was transiently detected only at 24 hours, consistently with a marginal activation of p53. Moreover, in contrast to ST1926-induced upregulation of Bax in parental cells, drug treatment caused a slight downregulation of Bax in R9A cells, clearly evident after prolonged exposure. Bcl-2 expression was not modulated by treatment in both cell lines. An early (6 hours) upregulation of p73 was detected in H460 cells, whereas no modulation of p73 expression could be detected in resistant cells even with high (equitoxic) drug concentrations (Figure 8*B*). p53 phosphorylation could be detected in resistant cells at concentrations 50- to 100-fold higher than in parental cells. This finding was consistent with the different extent of DNA damage found in the two cell lines.

We examined the expression of TR3, another transcription factor described to be upregulated by DNA damage and to be involved in the induction of apoptosis through the mitochondrial pathway [21]. Again, in contrast to the R9A cell line, H460 cells revealed an early upregulation of TR3 transcripts most evident after 6 hours of treatment (Figure 9).

Modulation of AKT and MAP Kinases

Because a differential basal or drug-induced activation of Akt and MAP kinases, which are involved in pathways regulating proliferation, survival, or apoptosis, might be determinant in the cell sensitivity to drug treatment, the state of activation of Akt and ERKs, JNKs, and p38 was examined in H460 and ST1926-resistant R9A cells. The drug effects were compared using equitoxic or equivalent concentrations. Cells were exposed for 6 hours to concentrations of ST1926 corresponding to IC_{50} and IC_{80} values for H460 cells (0.06 and 0.2 μM, respectively) and resistant cells (12 and 20 μM, respectively). Cell lysates were analyzed by Western blot analysis by the use of phospho-specific antibodies detecting the activated kinases. In spite of a reduced Akt expression in the resistant cells, Akt phosphorylation was similar in the two cell lines. ST1926 treatment did not affect Akt activation or expression (Figure 10). Similarly, activation of the ERKs was not modulated by the drug. However, whereas the protein expression of ERKs was similar in the two cell lines, the extent of basal

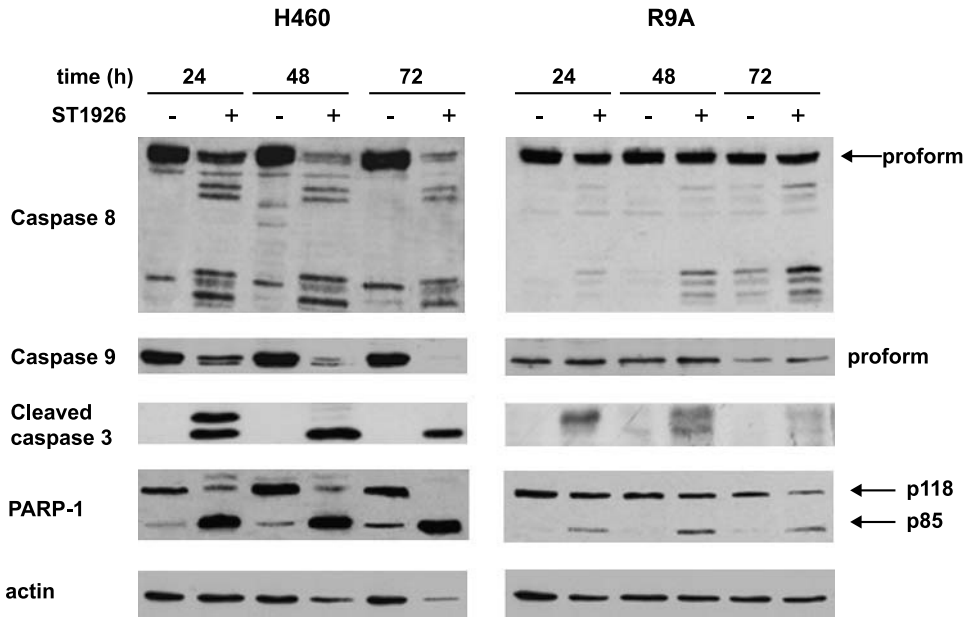

Figure 5. *Cleavage of caspases and PARP-1 in cells exposed to ST1926. Western blot analysis with specific antibodies was performed after 24, 48, and 72 hours of exposure to 0.2 μM and 20 μM ST1926 in H460 and R9A cells, respectively (IC_{80} at 72 hours). Actin is shown as a control for protein loading.*

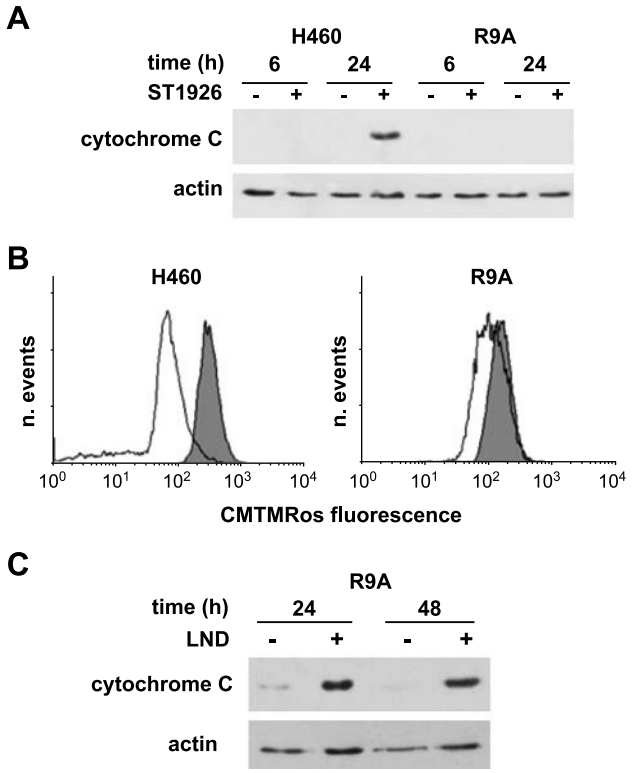

Figure 6. *Effect of ST1926 (A) or LND (C) on the release of cytochrome C into the cytosol. In (A), the two cell lines were exposed to equitoxic concentrations (IC_{80}) of ST1926; in (C), R9A cells were exposed to the IC_{80} value of LND (155 μM). The cytosolic extracts were prepared after the indicated times of drug exposure. (B) Analysis of mitochondrial transmembrane potential in H460 and R9A cells treated with ST1926 at their respective IC_{80} values. Cells were labeled with CMTMRos 24 hours after treatment with solvent (grey) or ST1926 (white), and then analyzed by flow cytometry to measure changes in $\Delta\psi_m$ (see Materials and Methods section for details).*

phosphorylation was consistently higher in R9A cells than in the parental cells. Atypical retinoids, including ST1926, have been reported to activate the stress MAP kinases, p38 and JNKs [9]. H460 and R9A cells did not differ in terms of expression or phosphorylation of these kinases in the absence of the drug. However, a dose-dependent activation of either p38 or JNK2 was induced by ST1926 only in the sensitive H460 cells, whereas no activation of stress kinases could be detected in R9A cells, even when treated with equitoxic concentrations of ST1926.

Discussion

The comparison of ST1926 effects on sensitive and resistant lung carcinoma cells indicates a substantially different pattern of cellular response and provides additional insights into the critical molecular events involved in antiproliferative/proapoptotic activities of adamantyl atypical retinoids. The most relevant observations of the present study are: 1) the selective resistance of the subline R9A to ST1926 was associated with a reduced and delayed apoptosis, and did not implicate a reduced uptake of the drug; 2) the resistance to the antiproliferative effects of ST1926 was accompanied by a lower induction of genotoxic stress; however, equitoxic drug concentrations produced a comparable extent of DNA damage in the two cell lines; 3) under equitoxic conditions, DNA damage response and cellular stress response, clearly evident in sensitive cells, were barely detectable in the resistant cells; and 4) the reduced susceptibility to apoptosis of R9A cells was associated with a lack of activation of the intrinsic mitochondrial-regulated pathway.

Our data indicate that in parental H460 cells, ST1926-induced apoptosis involved caspases 3, 9, and 8, thus implicating both intrinsic and extrinsic pathways of apoptosis. It is conceivable that the two cascades converge, resulting in a prompt and efficient cell death. In contrast, in resistant cells, no evidence was found of caspase 9 activation, but only a weak activation of caspases 8 and 3. This pattern of response suggests a lack of contribution of the mitochondrial-regulated apoptotic pathway. This interpretation was also supported by a lack of either cytochrome *C* release or mitochondrial transmembrane depolarization in resistant cells. Thus, in spite of the presence of a functional cell death receptor–mediated pathway in resistant cells, as suggested by the sensitivity to TRAIL, the available results support that the reduced susceptibility to ST1926-induced apoptosis could be the consequence of a loss of cooperation between the intrinsic and extrinsic pathways. Accordingly, a synergistic interaction between ST1926 and TRAIL was observed in H460 parental cells, but not in R9A cells.

Several lines of evidence indicate that CD437 and other related compounds induce apoptosis in a retinoid receptor–independent manner [2]. Synthetic derivatives of a novel

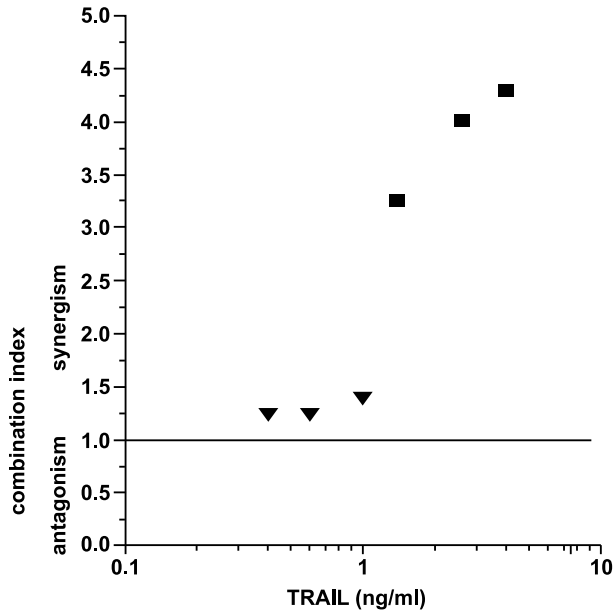

Figure 7. *Combination index (Drewinko index) for the interaction between ST1926 and TRAIL. H460 (■) and R9A (▼) cells were exposed to each drug or combination for 24 hours, using a single equitoxic concentration of ST1926 (i.e., 0.08 μM and 8 μM for H460 and R9A cells, respectively). The antiproliferative effect was determined after a 48-hour incubation in drug-free medium.*

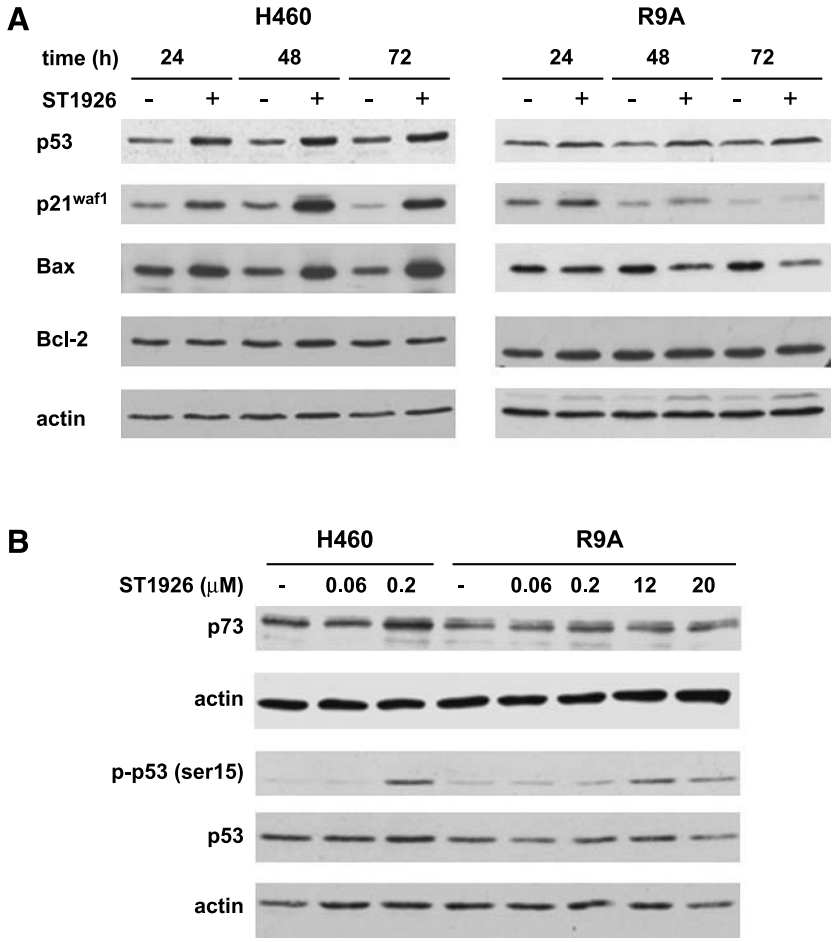

Figure 8. *(A) Expression of p53, p21^{WAF1}, Bax, and Bcl-2 in ST1926-sensitive (H460) and ST1926-resistant (R9A) cells treated with solvent (−) or ST1926 at the respective IC_{80} (+), for the indicated times. (B) Effect of ST1926 on p73 expression and p53 phosphorylation (Ser15) after cell exposure for 6 hours to both equivalent and equitoxic concentrations, corresponding to the respective IC_{50} and IC_{80} values. Whole-cell extracts were prepared and analyzed by Western blot analysis. Actin is shown as a control of protein loading.*

series, including ST1926 and MM002, display a low ability to activate RARγ, and are characterized by an almost complete loss of typical retinoid features [4,8,22]. Although a number of potential targets for apoptosis induction have been identified, the precise mechanism of action of adamantyl atypical retinoids remains unclear at the molecular level. Multiple mechanisms have been described in different tumor cells [5] and it is possible that the relevance of the reported effects is cell type–specific. In a number of cell lines derived from solid tumors, a typical feature of cellular response to ST1926 exposure is a marked activation of p53 [7,9]. It is well known that several stress stimuli, including genotoxic stress, activate p53 and induce apoptosis through p53-mediated upregulation of proapoptotic factors.

In a previous study performed in an ovarian carcinoma cell system, we have documented that ST1926 induces a significant extent of DNA breaks after a short-term exposure to the retinoid [9]. DNA adduct formation by CD437 has been reported [3,23]. The nature of the genotoxic stress, also detected in ST1926-treated H460 cells, is unknown, but it could not be ascribed to oxidative stress because the cellular effects of the drug were not modified by the use of antioxidant agents (not shown). The presence of genotoxic stress was supported by the pattern of cellular response, as documented by activation of p53 and p73, upregulation of p21 and Bax, and cell cycle arrest at the S-phase checkpoint in H460-sensitive cells. This response, together with activation of caspase 9 implicated in the mitochondrial-regulated pathway, is consistent with a p53-dependent apoptosis. Our study indicated that the induction of appreciable DNA breaks

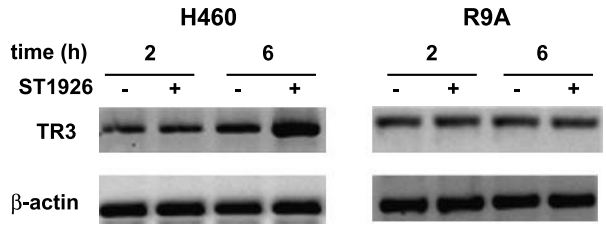

Figure 9. *RT-PCR analysis of TR3 expression in H460 and R9A cell lines. RNA was isolated after 2 or 6 hours of treatment with solvent (−) or ST1926 (0.2 μM for H460 and 20 μM for R9A cells). Amplification products with primers for TR3 and β-actin, separated on agarose gel, are shown.*

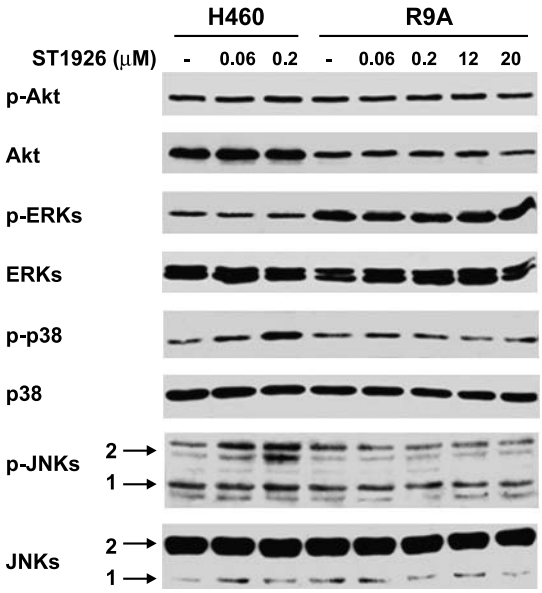

Figure 10. *Modulation of MAPKs and Akt by ST1926 in H460 and R9A cells. Cells were treated with solvent (−) or ST1926 at the indicated concentrations for 6 hours. Whole-cell lysates were processed for Western blot analysis using phospho-specific antibodies to detect the activated kinases. Protein expression was controlled by specific antiprotein antibodies.*

by drug treatment was substantially reduced in resistant cells. Indeed, DNA breaks were detectable in resistant cells only at cytotoxic concentrations, thus supporting the relevance of genotoxic stress in the mechanism of drug action. In spite of recognition of DNA lesions, as evidenced by drug-induced formation of γ-H2AX foci and p53 phosphorylation, the resistant cells were characterized by a deficient DNA damage response, as indicated by a loss of cell cycle arrest at DNA damage checkpoint during DNA synthesis and by a marginal activation of cell death pathways, resulting in cellular tolerance to the genotoxic stress.

The lack of activation of the mitochondrial pathway of cell death in resistant cells could not be ascribed to a defect in the mitochondrial functions because LND, a mitochondrial targeting drug, was effective as apoptosis inducer. The alterations associated with the resistant phenotype, including marginal activation of p53 and p21, lack of activation of p73, and downregulation of Bax, support a defective DNA damage signaling occurring upstream of the mitochondria. The lack of drug-induced transcription of TR3 in resistant cells is also consistent with this interpretation because TR3 functions as a proapoptotic factor by interaction with mitochondrial membrane [24–26]. The mechanism by which atypical retinoids induce TR3 is not fully understood. In previous studies, the upregulation of TR3 by CD437 has been ascribed to MEF2 or c-*jun* activation mediated by p38 or JNK, respectively [21,27]. However, no definitive explanation for the activation of cellular stress response has been provided [28]. The observation that TR3 expression can be induced by a variety of stimuli, including DNA damage, is worth noting [29,30].

The activation of stress-inducible molecules, such as JNK and p38, is part of a cellular response to genotoxic stress [31]. Although JNK may be implicated in some forms of apoptotic cell death, depending on the biologic context [32], activation of signaling pathways involving MAPK by DNA-damaging agents likely reflects a protective response [33,34]. Such a similar role has been documented in ovarian carcinoma cells because inhibition of stress-activated kinases resulted in an enhancement of ST1926-induced apoptosis [9]. In the drug-sensitive ovarian carcinoma cell line, the pattern of cellular response to the atypical retinoid, ST1926, was comparable to that observed in H460 cells in terms of activation of DNA damage response and modulation of proteins/genes implicated in genotoxic stress, including the activation and upregulation of AP-1 transcription factors. The latter event reflects the activation of stress-activated MAPK pathways. cDNA array analysis of transcription in H460 cell provided evidence of increased expression of c-*jun*, a member of AP-1 complex (not shown). Thus, modulation of AP-1 complex appears to involve not only phosphorylation of the protein but also enhanced transcription. Again, this modulation likely reflects a protective cellular response to the genotoxic stress because the activation of AP-1 transcription factors has been already described following treatment with other genotoxic agents (e.g., UV radiation) and is mediated by stress-activated protein kinases [35]. In addition, in the present study, cytotoxic concentrations of ST1926 are shown to induce an appreciable apoptosis also in resistant R9A cells without activating JNKs and p38, thereby suggesting that stress kinases did not mediate ST1926-induced apoptotic signals in the H460 cell system. The alterations responsible for resistance to apoptosis in R9A cells mapped upstream of events inducing the activation of JNK/p38 and the induction of the intrinsic apoptotic pathway. In addition, the high basal activation of the ERKs in R9A cells might also contribute to the resistant phenotype as a component of a survival pathway [36].

In conclusion, the development of resistance in H460 cells reflects alterations in the mechanisms involved in the drug induction of DNA lesions and in cellular response to the genotoxic stress. The attenuated DNA damage response and the absence of stress response to cytotoxic concentrations of ST1926 in resistant cells are consistent with the interpretation that resistant cells might be defective in signal transduction pathways triggered by the genotoxic lesions.

Acknowledgement

The authors thank Laura Zanesi for editorial assistance.

References

[1] Fontana JA and Rishi AK (2002). Classical and novel retinoids: their targets in cancer therapy. *Leukemia* **16,** 463–472.

[2] Lotan R (2003). Receptor-independent induction of apoptosis by synthetic retinoids. *J Biol Regul Homeost Agents* **17,** 12–28.

[3] Zhao X and Spanjaard RA (2003). The apoptotic action of the retinoid CD437/AHPN: diverse effects, common basis. *J Biomed Sci* **10,** 44–49.

[4] Garattini E, Gianni M, and Terao M (2004). Retinoid related molecules an emerging class of apoptotic agents with promising therapeutic

potential in oncology: pharmacological activity and mechanisms of action. *Curr Pharm Des* **10,** 433–448.

[5] Sun S-Y, Yue P, and Lotan R (2000). Implication of multiple mechanisms in apoptosis induced by the synthetic retinoid CD437 in human prostate carcinoma cells. *Oncogene* **19,** 4513–4522.

[6] Hail N, Youssef EM, and Lotan R (2001). Evidence supporting a role for mitochondrial respiration in apoptosis induction by the synthetic retinoid CD437. *Cancer Res* **61,** 6698–6702.

[7] Sun S-Y, Yue P, Chen X, Hong WK, and Lotan R (2002). The synthetic retinoid CD437 selectively induces apoptosis in human lung cancer cells while sparing normal human lung epithelial cells. *Cancer Res* **62,** 2430–2436.

[8] Cincinelli R, Dallavalle S, Merlini L, Penco S, Pisano C, Carminati P, Giannini G, Vesci L, Gaetano C, Illy B, et al. (2003). A novel atypical retinoid endowed with proapoptotic and antitumor activity. *J Med Chem* **46,** 909–912.

[9] Zuco V, Zanchi C, Cassinelli G, Lanzi C, Supino R, Pisano C, Zanier R, Giordano V, Garattini E, and Zunino F (2004). Induction of apoptosis and stress response in ovarian carcinoma cell lines treated with ST1926, an atypical retinoid. *Cell Death Differ* **11,** 280–289.

[10] Garattini E, Parrella E, Diomede L, Gianni M, Kalac Y, Merlini L, Simoni D, Zanier R, Fosca Ferrara F, Chiarucci I, et al. (2004). ST1926, a novel and orally active retinoid-related molecule inducing apoptosis in myeloid leukemia cells: modulation of intracellular calcium homeostasis. *Blood* **103,** 194–207.

[11] Drewinko B, Loo TL, Brown JA, Gottlieb JA, and Freireich EJ (1976). Combination chemotherapy *in vitro* with adriamycin. Observations of additive, antagonistic, and synergistic effects when used in two-drug combination on cultured human lymphoma cells. *Cancer Biochem Biophys* **1,** 187–195.

[12] Kohn KW, Ewig RAG, Erickson LC, and Zwelling LA (1981). DNA repair. In Friedberg EC, Hanawalt PC (Eds.), A Laboratory Manual of Research Procedures (Part B), Vol. 1, pp. 370–401 Marcel Dekker, New York.

[13] Milner AE, Palmer DH, Hodgkin EA, Eliopoulos AG, Knox PG, Poole CJ, Kerr DJ, and Young LS (2002). Induction of apoptosis by chemotherapeutic drugs: the role of FADD in activation of caspase-8 and synergy with death receptor ligands in ovarian carcinoma cells. *Cell Death Differ* **9,** 287–300.

[14] Bossy-Wetzel E, Newmeyer DD, and Green DR (1998). Mitochondrial cytochrome *C* release in apoptosis occurs upstream of DEVD-specific caspase activation and independently of mitochondrial transmembrane depolarization. *EMBO J* **17,** 37–49.

[15] Modesti M and Kanaar R (2001). DNA repair: spot(light)s on chromatin. *Curr Biol* **11,** R229–R232.

[16] Taneja N, Davis M, Choy JS, Beckett MA, Singh R, Kron SJ, and Weichselbaum RR (2004). Histone H2AX phosphorylation as a predictor of radiosensitivity and target for radiotherapy. *J Biol Chem* **279,** 2273–2280.

[17] Huang X, Traganos F, and Darzynkiewicz Z (2003). DNA damage induced by DNA topoisomerase I- and topoisomerase II-inhibitors detected by histone H2AX phosphorylation in relation to the cell cycle phase and apoptosis. *Cell Cycle* **2,** 614–619.

[18] Wang H, Guan J, Wang H, Perrault AR, Wang Y, and Iliakis G (2001). Replication protein A2 phosphorylation after DNA damage by the coordinated action of ataxia telangiectasia–mutated and DNA-dependent protein kinase. *Cancer Res* **61,** 8554–8563.

[19] Ravagnan L, Marzo I, Costantini P, Susin SA, Zamzami N, Petit PX, Hirsch F, Goulbern M, Poupon MF, Miccoli L, et al. (1999). Lonidamine triggers apoptosis *via* a direct, Bcl-2–inhibited effect on the mitochondrial permeability transition pore. *Oncogene* **18,** 2537–2546.

[20] Costantini P, Jacotot E, Decaudin D, and Kroemer G (2000). Mitochondrion as a novel target of anticancer chemotherapy. *J Natl Cancer Inst* **92,** 1042–1053.

[21] Holmes WF, Soprano DR, and Soprano KJ (2003). Early events in the induction of apoptosis in ovarian carcinoma cells by CD437: activation of the p38 MAP kinase signal pathway. *Oncogene* **22,** 6377–6386.

[22] Zhang Y, Dawson MI, Mohammad R, Rishi AK, Furhana L, Feng K-C, Leid M, Peterson V, Zhang X, Edelstein M, et al. (2002). Induction of apoptosis of human B-CLL and ALL cells by a novel retinoid and its nonretinoidal analog. *Blood* **100,** 2917–2925.

[23] Zhao X, Demary K, Wong L, Vaziri C, McKenzie AB, Eberlein TJ, and Spanjaard RA (2001). Retinoic acid receptor–independent mechanism of apoptosis of melanoma cells by the retinoid CD437 (AHPN). *Cell Death Differ* **8,** 878–886.

[24] Li H, Kolluri SK, Gu J, Dawson MI, Cao X, Hobbs PD, Lin B, Chen G, Lu J, Lin F, et al. (2000). Cytochrome *C* release and apoptosis induced by mitochondrial targeting of nuclear orphan receptor TR3. *Science* **289,** 1159–1164.

[25] Holmes WF, Soprano DR, and Soprano KJ (2003). Comparison of the mechanism of induction of apoptosis in ovarian carcinoma cells by the conformationally restricted synthetic retinoids CD437 and 4-HPR. *J Cell Biochem* **89,** 262–278.

[26] Dawson MI, Hobbs PD, Peterson VJ, Leid M, Lange CW, Feng K-C, Chen G, Gu J, Li H, Kolluri K, et al. (2001). Apoptosis induction in cancer cells by a novel analogue of 6-[3-(1-adamantyl)-4-hydroxyphenyl]-2-nephthalenecarboxylic acid lacking retinoid receptor transcriptional activation activity. *Cancer Res* **61,** 4723–4730.

[27] Li Y, Lin B, Agadir A, Liu R, Dawson MI, Reed JC, Fontana JA, Bost F, Hobbs PD, Zheng Y, et al. (1998). Molecular determinants of AHPN (CD437)–induced growth arrest and apoptosis in human lung cancer cell lines. *Mol Cell Biol* **18,** 4719–4731.

[28] Pfahl M and Piedrafita FJ (2003). Retinoid targets for apoptosis induction. *Oncogene* **22,** 9058–9062.

[29] Brenner C and Kroemer G (2000). Mitochondria—the death signal integrators. *Science* **289,** 1150–1151.

[30] Liu S, Wu Q, Ye XF, Cai JH, Huang ZW, and Su WJ (2002). Induction of apoptosis by TPA and VP-16 is through translocation of TR3. *World J Gastroenterol* **8,** 446–450.

[31] Martindale JL and Holbrook NJ (2002). Cellular response to oxidative stress: signaling for suicide and survival. *J Cell Physiol* **192,** 1–15.

[32] Herr I and Debatin KM (2001). Cellular stress response and apoptosis in cancer therapy. *Blood* **98,** 2603–2614.

[33] Levresse V, Marek L, Blumberg D, and Heasley LE (2002). Regulation of platinum-compound cytotoxicity by the c-Jun N-terminal kinase and c-Jun signaling pathway in small-cell lung cancer cells. *Mol Pharmacol* **62,** 689–697.

[34] Gjerset RA, Lebedeva S, Haghighi A, Turla ST, and Mercola D (1999). Inhibition of the Jun kinase pathway blocks DNA repair, enhances p53-mediated apoptosis and promotes gene amplification. *Cell Growth Differ* **10,** 545–554.

[35] Tanos T, Marinissen MJ, Leskow FC, Hochbaum D, Martinetto H, Gutkind JS, and Coso OA (2005). Phosphorylation of c-Fos by members of the p38 MAPK family: role in the AP-1 response to UV. *J Biol Chem* (in press).

[36] Dent P, Yacoub A, Fisher PB, Hagan MP, and Grant S (2003). MAPK pathways in radiation responses. *Oncogene* **22,** 5885–5896.